JACS
JOURNAL OF THE AMERICAN CHEMICAL SOCIETY

COMMUNICATION

pubs.acs.org/JACS

Template-Directed Synthesis of Ordered Single-Crystalline Nanowires Arrays of Cu_2ZnSnS_4 and $Cu_2ZnSnSe_4$

Liang Shi,*[†] Congjian Pei,[‡] Yeming Xu,[‡] and Quan Li*[‡]

[†]Department of Chemistry, University of Science and Technology of China, Hefei 230026, P. R. China

[‡]Department of Physics, The Chinese University of Hong Kong, Shatin, New Territory, Hong Kong, P. R. China

Supporting Information

ABSTRACT: Highly ordered quaternary semiconductor Cu_2ZnSnS_4 nanowires array have been prepared via a facile solvothermal approach using anodic aluminum oxide (AAO) as a hard template. The as-prepared nanowires are uniform and single crystalline. They grow along either the crystalline $[1\bar{1}0]$ or $[11\bar{1}]$ direction. The structure, morphology, composition, and optical absorption properties of the as-prepared Cu_2ZnSnS_4 samples were characterized using X-ray powder diffraction, transmission electron microscopy, energy dispersive X-ray spectrometry, scanning electron microscopy, and UV−vis spectrometry. A possible formation mechanism of the nanowire arrays is proposed. Governed by similar mechanism, we show that $Cu_2ZnSnSe_4$ nanowire array with similar structural characteristics can also be obtained.

As important copper-based quaternary chalcopyrite semiconductors, Cu_2ZnSnS_4 (CZTS) and $Cu_2ZnSnSe_4$ (CZTSe) have attracted increasing attention in recent years because they are the most promising low cost alternatives to conventional solar cell materials. Both of them have large absorption coefficients ($>10^4$ cm^{-1}) and direct band gaps (E_g = 1.0−1.5 eV) that match the preferred range of solar irradiation.[1−4] The crystal structures and optical properties of CZTS and CZTSe are similar to those of $Cu(In,Ga)Se_2$ (CIGS), an important solar cell material. Nevertheless, CIGS contains rare metals of In and Ga, which make it expensive. As a comparison, the composition of naturally abundant elements Sn and Zn makes CTZS and CZTSe particularly attractive, as such characteristic can enable the large-scale commercial application. In fact, it has been theoretically predicted that the power conversion efficiency can be as high as 32.2% for CZTS, a 6.77% efficiency has already been reached experimentally in thin film CZTS solar cells,[5] while an even higher efficiency of 9.66% has been achieved in CZTSe based solar cells.[6] Quinary combination CZTSSe was also used to for the development of low cost thin film solar cells with efficiency as high as 7.2%.[7]

Attracted by the economical advantage and excellent property of this family of materials, much research effort has been devoted to the synthesis of CZTS and CZTSe nanoparticles recently,[8−12] aiming at employing them for low cost photovoltaic devices by adopting the ink printing technology. Nevertheless, preparation of single crystalline CTZS and CZTSe nanowires in a well-aligned array configuration has not been reported to the best of our knowledge. Such chalcopyrite semiconductors in the nanowire morphology can offer a well-defined nanoscale domain with clearly identifiable grain boundaries, where an energy barrier exists and prevents charge carrier recombination.[13,14] In addition, the well-aligned nanowires may provide continuous charge carrier transport pathways without dead ends. These favorable characteristics would lead to increase in conversion efficiency in the nanowire photovoltaic devices.[15] In the present study, we report a facile solution approach with AAO as a hard template for preparation of arrays of well-aligned uniform single crystalline CZTS nanowires with elaboration on their formation mechanisms. Using similar growth methodologies, we demonstrate that $Cu_2ZnSnSe_4$ nanowire arrays can also be obtained with comparable structural/morphological characteristics as those of CZTS.

All reagents are analytical grade and used without further purification. AAO templates (Whatman Co., U.K.) with pore sizes of 200 nm in diameter were used in the experiments. In a typical procedure, a precursor solution (for CZTS and CZTSe) was prepared first in air with mild magnetic stirring. AAO template was then immersed in the precursor solution, followed by 5 min sonication to remove the air in the AAO pore. Afterward, the system was attached to a Schlenk line to purge oxygen and water under rough vacuum, followed by 10 min nitrogen bubbling. The evacuation and N_2 bubbling process was cycled for 3 times at room temperature. The solution was then transferred into a 20 mL stainless steel Teflon-lined autoclave. The autoclave was sealed and the temperature was maintained at 230 °C for 70 h before being cooled down to room temperature. The AAO template containing the product was taken out, thoroughly washed with ethanol and distilled water, and air-dried before characterization. For CZTS synthesis, the precursor solution contains 0.096 g of sulfur, 0.14 g of anhydrous CuCl, 0.14 g of $SnCl_2$, 0.1 g of $ZnCl_2$, and 16 mL of anhydrous ethylenediamine (En). In the case of CZTSe, 0.23 g of selenium powder is used instead of sulfur; other conditions remained unchanged.

The overall crystallinity of the product is examined by X-ray diffraction (XRD, Rigakau RU-300 with Cu Kα radiation). The general morphology of the products was characterized using scanning electron microscopy (FESEM QF400). Detailed microstructure analysis was carried out using transmission electron microscopy (TEM Tecnai 20ST). The chemical composition and the spatial distribution of the compositional elements in the product were examined using an energy dispersive X-ray (EDX) spectrometer and Gatan image filtering (GIF) system, attached to the same microscope. For the SEM measurements, several

Received: February 24, 2011
Published: June 17, 2011

dx.doi.org/10.1021/ja201740w | J. Am. Chem. Soc. 2011, 133, 10328–10331

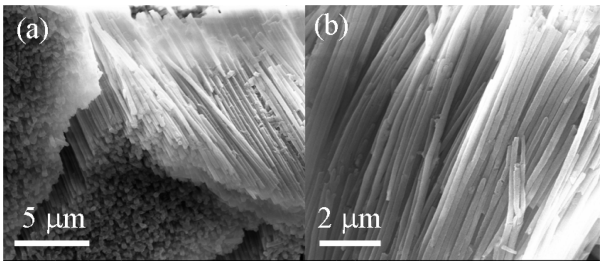

Figure 1. (a) Top view and (b) side view SEM images of the as-prepared Cu_2ZnSnS_4 nanowires array after etching off the AAO template.

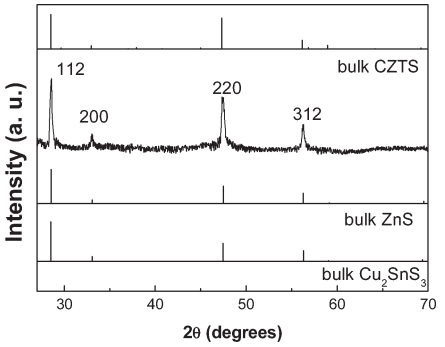

Figure 2. A representative XRD pattern of the as-prepared CZTS nanostructure.

drops of 1 M NaOH aqueous solution were added onto the sample to dissolve some part of the AAO template. The residual solution on the surface of the template was rinsed with distilled water. For the TEM and HRTEM measurements, the template was completely dissolved in 2 M NaOH aqueous solution. The product was centrifuged, thoroughly washed with distilled water to remove residual NaOH, and then rinsed with absolute ethanol.

After etching off the AAO template, highly ordered nanowire arrays can be observed. Figure 1 shows the SEM images taken from such a sample. The surfaces of the nanowires in array appear smooth. The length of the nanowires is in the range of several micrometers, and their average diameter is ~200 nm, being consistent with the pore size of the AAO template.

The crystalline structure of the product (embedded in the AAO template) was first characterized by XRD. All of the diffraction peaks (Figure 2) can be indexed to the tetragonal Cu_2ZnSnS_4 (JCPDS card, No. 26-0575). However, these peaks also coincide with diffractions from several other phases including the zinc blend ZnS (JCPDS card, No.5-0566) and tetragonal Cu_2SnS_3 (JCPDS card, No.894714), the standard diffractions of which are also plotted in Figure 2. Consequently, XRD itself fails to give conclusive evidence on the existence of phase pure tetragonal Cu_2ZnSnS_4.

Further structural information of the sample on macroscopic scale is obtained from Raman spectrum (Figure 3). A strong peak at 338 cm^{-1} and a weak peak at 287 cm^{-1}, agreeing well with those of bulk CZTS,[16] can be found in Figure 3. On the other hand, the characteristic Raman peak of zinc blende ZnS at 356 cm^{-1}[17] is absent in the spectrum, suggesting that the XRD diffractions should not result from such a phase.

Detailed characterizations of microstructure and chemical composition of individual nanowire are obtained using TEM-related techniques. Figure 4a shows the typical morphology of one nanowire, and EDX (Figure 4b) taken from such a wire suggests the coexistence of Cu, Zn, Sn, and S (Au TEM grid is employed to avoid background signal from conventional Cu grid). Quantitative analysis of the EDX data (Table S1) taken from different locations on a number of individual nanowires suggests the composition of such nanowire is close to the stoichiometry Cu_2ZnSnS_4 (Cn/Zn/Sn/S ~ 2.2/0.9/0.8/4.1). The spatial distribution of different compositional elements is obtained from the STEM-EDX elemental mapping. Figure 4c shows the dark field image of a portion of the single nanowire, and Figure 4d–g give the elemental maps of Cu, Zn, Sn, and S, respectively. Uniform distribution of all compositional elements is suggested from the experimental observation. Together with the XRD and Raman data, one can confirm that Cu_2ZnSnS_4 nanowires have been formed. Similar compositional and morphological characteristics can be found for the CZTSe nanowires (Figure S1–5).

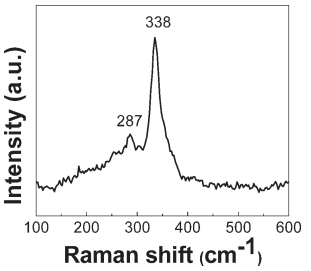

Figure 3. Room temperature Raman spectrum of the as-prepared nanostructures.

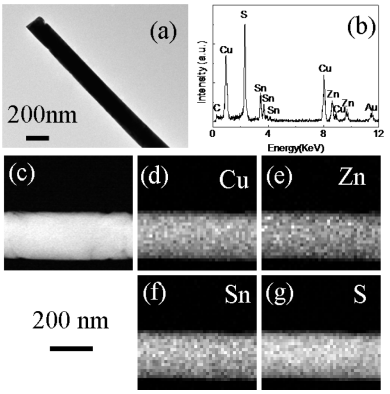

Figure 4. (a) Low magnification bright field image, and (b) EDX spectrum of the as-prepared Cu_2ZnSnS_4 nanowire; (c) dark field image of a portion of Cu_2ZnSnS_4 nanowire; (d–g) EDX elemental maps of Cu, Zn, Sn, S, respectively.

The crystallinity of individual nanowires is further analyzed using transmission electron microscopy, which has been carried out on several tens of different single nanowires. All of the nanowires examined are single crystalline, as suggested by both the selected area electron diffractions patterns (Figure S7) and high resolution images taken on these nanowires. Figure 5a,b gives the typical electron diffraction patterns of such CZTS nanowires, which can be indexed to the [221] zone axis of chalcopyrite CZTS. Two common growth directions have been identified for most of the nanowires examined, that is, they are

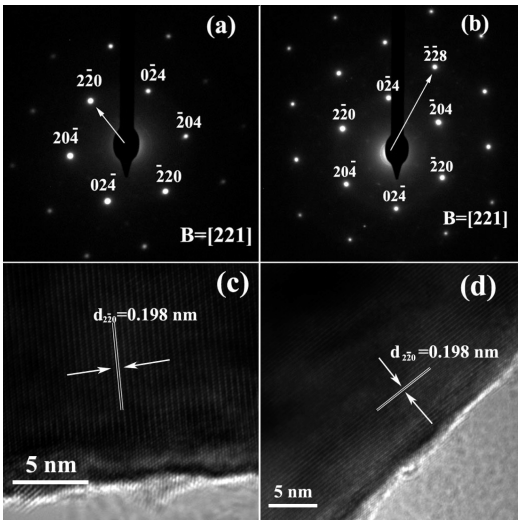

Figure 5. (a and b) Diffraction pattern of the as-prepared Cu_2ZnSnS_4 nanowires, the arrows indicate the nanowire growth directions, along $[1\bar{1}0]$ and $[11\bar{1}]$, respectively; (c and d) HRTEM images taken at the surface regions of two CZTS nanowires with the two different growth directions.

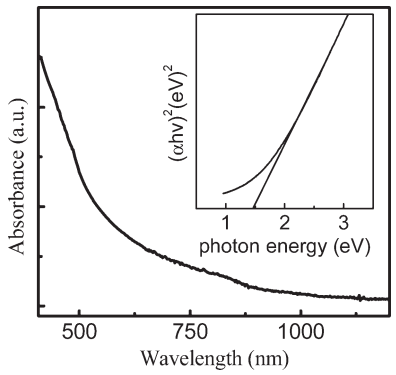

Figure 6. A typical room-temperature UV−visible absorption of the as-prepared Cu_2ZnSnS_4 nanowires.

grown along either the $[1\bar{1}0]$ (Figure 5a) or $[11\bar{1}]$ (Figure 5b) crystalline directions of CZTS, with the two of them being perpendicular to each other. Such a growth manner is also confirmed by the high resolution images taken from the corresponding nanowires—one can see the one in Figure 5c grows along the $[1\bar{1}0]$ direction, with its $(2\bar{2}0)$ planes being perpendicular to the growth direction; and another one in Figure 4d, with its $(2\bar{2}0)$ planes being parallel to the growth direction. Statistical analysis of the growth direction suggests 80% of the nanowires grow along the $[11\bar{1}]$ direction, based on several tens of nanowires examined.

Figure 6 shows the room temperature UV−vis absorption spectrum for the as-prepared Cu_2ZnSnS_4 nanowires sample. The sample appears black due to the strong photon absorption in the entire visible range of light, suggesting their potential in solar energy conversation applications. Estimation on the optical band gap (E_g) of the Cu_2ZnSnS_4 nanowires can be obtained by plotting $(\alpha h\nu)^2$ as a function of the photon energy (in the inset of Figure 6), with α being the absorption coefficient, h Planck's constant, and ν the frequency. The E_g value is estimated as 1.5 eV from the intersection of the extrapolated linear portion with the x-axis (photon energy), being consistent with the reported values of Cu_2ZnSnS_4 in literature (1.45−1.51 eV).[18,19] Such band gap value is desirable for the photovoltaic and photocatalytic applications. The optical property of the CZTSe nanowires is very similar to that of the CZTS, and ~1.3 eV has been estimated as its band gap energy from the corresponding absorption spectrum (Figure S6).

The similar morphological/structural characteristics of CZTS and CZTSe suggest their growth is governed by similar principles. We shall take CZTS as an example to discuss its formation mechanism, which should be divided into the nucleation and growth stage. Chemically, the choice of ethylenediamine (En) as solution is critical for Cu_2ZnSnS_4 nucleation. Ethylenediamine is known as a strong chelating agent. It not only chelates with Cu^+, Sn^{2+}, and Zn^{2+} to form complex ions, but also serves as good solvent for sulfur.[20] The dissolved elemental S is soon reduced to S^{2-} by an organic nucleophilic attack, and the reaction between the S^{2-} and the complex ions (composed of the En chelated Cu^+, Sn^{2+}, Zn^{2+}) initiates the nucleation of Cu_2ZnSnS_4.

Two possible nucleation mechanisms exist when AAO template is employed. If the interactions between reagent molecules are stronger than those between the reagent molecules and the AAO pore walls, homogeneous nucleation would occur within the voluminous pores. Otherwise, heterogeneous nucleation would take place on the AAO pore walls. In the present study, the pore walls of AAO were positively charged due to the presence of a layer of acidic anions either held covalently or present as hydrated anions (complex anions $Al(H_2O)_4(OH)^+_2$ and $Al(H_2O)_4^+$) .[21] At the same time, the formed complex ions composed of En chelated Cu^+, Sn^{2+}, Zn^{2+} are also positively charged. Consequently, homogeneous nucleation would be preferred as the pore wall would repel the En chelated complex ions. In fact, one would expect the formation of Cu_2ZnSnS_4 nanotube at short growth duration if heterogeneous nucleation takes the lead, while Cu_2ZnSnS_4 nanowire should always be observed if otherwise. A time dependent Cu_2ZnSnS_4 growth discloses that Cu_2ZnSnS_4 nanowire is always formed and independent of the growth duration (Figure S8). This serves as another piece of supportive evidence for the homogeneous nucleation.

Grain growth always follows the nucleation process, while a competition between nucleation and growth also exists. The time dependent growth experiment revealed an interesting polycrystalline-to-single crystalline evolution for the Cu_2ZnSnS_4 nanowire. We have found multiple nanocrystals start to fill in the pores of AAO template at short growth durations (<12 h). They are so loosely attached to each other that the "nanowire" morphology cannot be maintained after removal of the AAO template. Increasing the growth duration results (<36 h) in polycrystalline nanowires with loose structure, although these polycrystalline nanowires become more and more dense for longer growth durations (Figure S8c,e). Single crystalline nanowires start to appear for sample grown for 48 h, and by then the contrast from polycrystalline grains (in bright field TEM image) completely disappears, and the selected area diffraction pattern shows characteristics of single crystal (Figure S8 (h)). This experimental observation suggest that multiple homogeneous nucleation occur simultaneously within the voluminous AAO pores, and the single crystallinity of the nanowires was achieved via specific route other than single seed growth. One possible mechanism is the classical Ostwald-ripening—bigger crystals grow at the

expense of smaller ones, which theory has been successfully used to explain the diffusion-controlled crystal growth process. Oriented attachment serves another possible mechanism—smaller particles with common crystallographic orientations directly combine to form larger ones by crystallographic fusion at the planar interface. This mechanism is also known as the grain-rotation-induced grain coalescence (GRIGC) mechanism[22,23] because the collided random particles with no common crystallographic orientation tend to rotate into common orientation to obtain the structural accord at their interface. As a result, coherent grain−grain boundary is formed and disappears when a single larger nanocrystal is produced. Considering the length scale of the nanowires and their single crystallinity over such a length scale, the oriented attachment mechanism provides a better explanation for the Cu_2ZnSnS_4 nanowire growth in the present study. The observed preferred growth direction might be related to the minimization of the surface energy of the nanowires, which is currently under investigation.

In conclusion, a facile solution approach for fabrication of large-scale quaternary Cu_2ZnSnS_4 and $Cu_2ZnSnSe_4$ nanowire array has been developed. During the reaction process, AAO was used as a morphology directing template and ethylenediamine acted as both a reducing agent and an effective chelating agent. A growth mechanism of the nanowire array was also proposed. UV−vis optical properties suggested band-gaps of ∼1.5 and ∼1.3 eV for the as-prepared CZTS and CZTSe nanowires, respectively, disclosing their suitability for the photovoltaic application. We believe highly ordered array of other one-dimensional nanostructured quaternary chalcopyrite can also be obtained using the current synthesis approach. Related further research works are underway.

■ ASSOCIATED CONTENT

Supporting Information. Detailed information on characterization of $Cu_2ZnSnSe_4$ single crystalline nanowire array, including XRD pattern, Raman spectrum, SEM and TEM images, UV−visible absorbance spectrum and EDX elemental mapping images for Cu, Zn, Sn, Se. Information on time dependent Cu_2ZnSnS_4 growth process and SAED patterns along the length of a Cu_2ZnSnS_4 single nanowire is also included. This material is available free of charge via the Internet at http://pubs.acs.org.

■ AUTHOR INFORMATION

Corresponding Author
sliang@ustc.edu.cn; liquan@phy.cuhk.edu.hk

■ ACKNOWLEDGMENT

This work was supported by the National Natural Science Foundation of China (No. 21071135) and Q.L. acknowledge the funding from GRF under project No. 414709, 414908 and 414710.

■ REFERENCES

(1) Katagiri, H. *Thin Solid Films* **2005**, *480*, 426.
(2) Jimbo, K.; Kimura, R.; Kamimura, T.; Yamada, S.; Maw, W. S.; Araki, H.; Oishi, K.; Katagiri, H. *Thin Solid Films* **2007**, *515*, 5997.
(3) Shavel, A.; Arbiol, J.; Cabot, A. *J. Am. Chem. Soc.* **2010**, *132*, 4514.
(4) Grossberg, M.; Krustok, J.; Timmo, K.; Altosaar, M. *Thin Solid Films* **2009**, *517*, 2489.
(5) Katagiri, H.; Jimbo, K.; Maw, W. S.; Oishi, K.; Yamazaki, M.; Araki, H.; Takeuchi, A. *Thin Solid Films* **2009**, *517*, 2455.
(6) Todorov, T. K.; Reuter, K. B.; Mitzi, D. B. *Adv. Mater.* **2010**, *22*, 1.
(7) Guo, Q. J.; Ford, G. M.; Yang, W. C.; Walker, B. C.; Stach, E. A.; Hillhouse, H. W.; Agrawal, R. *J. Am. Chem. Soc.* **2010**, *132*, 17384.
(8) Guo, Q. J.; Hillhouse, H. W.; Agrawal, R. *J. Am. Chem. Soc.* **2009**, *131*, 11672.
(9) Steinhagen, C.; Panthani, M. G.; Akhavan, V.; Goodfellow, B.; Koo, B.; Korgel, B. A. *J. Am. Chem. Soc.* **2009**, *131*, 12554.
(10) Riha, S. C.; Parkinson, B. A.; Prieto, A. L. *J. Am. Chem. Soc.* **2009**, *131*, 12054.
(11) Wei, H.; Ye, Z. C.; Li, M; Su, Y. J.; Yang, Z; Zhang, Y. F. *CrystEngComm* **2011**, *13*, 2222.
(12) Haas, W.; Rath, T.; Pein, A.; Rattenberger, J.; Trimmel, G.; Hofer, F. *Chem. Commun.* **2011**, *47*, 2050.
(13) Hetzer, M. J.; Strzhemechny, Y. M.; Gao, M.; Contreras, M. A.; Zunger, A.; Brillson, L. J. *Appl. Phys. Lett.* **2005**, *86*, 162105.
(14) Peng, H.; Schoen, D. T.; Meister, S. X.; Zhang, F.; Cui, Y. *J. Am. Chem. Soc.* **2007**, *129*, 34.
(15) Persson, C.; Zunger, A. *Phys. Rev. Lett.* **2003**, *91*, 266401.
(16) Himmrich, M.; Haeuseler, H. *Spectrochim. Acta A, Mol. Spectrosc.* **1991**, *47*, 933.
(17) Fernandes, P. A.; Salome, P. M. P.; da Cunha, A. F. *Thin Solid Films* **2009**, *517*, 2519.
(18) Ito, K.; Nakazawa, T. *Jpn. J. Appl. Phys., Part 1* **1988**, *27*, 2094.
(19) Katagiri, H. *Thin Solid Films* **2005**, *480*, 426.
(20) Ma, X.; Xu, F.; Liu, Y.; Liu, X.; Zhang, Z.; Qian, Y. *Mater. Res. Bull.* **2005**, *40*, 2180.
(21) Diggle, J. W.; Downie, T. C.; Goulding, C. W. *Chem. Rev.* **1969**, *69*, 365.
(22) Leite, E. R.; Giraldi, T. R.; Pontes, F. M.; Longo, E.; Beltran, A.; Andr_es, J. *Appl. Phys. Lett.* **2003**, *83*, 1566.
(23) Moldovan, D.; Yamakov, V.; Wolf, D.; Phillpot, S. R. *Phys. Rev. Lett.* **2002**, *89*, 206101.